การประชุมวิชาการเครือข่ายวิศวกรรมเครื่องกลแห่งประเทศไทยครั้งที่ 14
2-3 พฤศจิกายน 2543 โรงแรม โนโวเทล เชียงใหม่

การทดสอบความล้าแบบควบคุมความเครียดโดยใช้ระบบตรวจวัดภาพแบบดิจิตอล

Non-Contact Strain-Controlled Fatigue Test with Digital Image Measurement System

ชาวสวน กาญจโนมัย[1], ชินอิจิ ยามาโมโต้[2], ยูกิ มิยาชิตะ[2] และ โยชิฮารุ มูโต้[2]

1- ภาควิชาวิศวกรรมเครื่องกล คณะวิศวกรรมศาสตร์ มหาวิทยาลัยธรรมศาสตร์ ปทุมธานี 12121

2- ภาควิชาวิศวกรรมเครื่องกล มหาวิทยาลัยนากาโอกะ นีกาตะ 940-2188 ประเทศญี่ปุ่น

C. Kanchanomai[1], S. Yamamoto[2], Y. Miyashita[2] and Y. Mutoh[2]

1 - Department of Mechanical Engineering, Thammasat University, Patumthani 12121, Thailand

2 - Department of Mechanical Engineering, Nagaoka University of Technology, Nagaoka-shi 940-2188, Japan

Email: chaosuan@stn.nagaokaut.ac.jp

บทคัดย่อ

ระบบตรวจวัดภาพแบบดิจิตอลถูกนำมาใช้ควบคุมการเปลี่ยนแปลงระยะของชิ้นทดลองในการทดสอบความล้า ซึ่งสามารถที่จะหลีกเลี่ยงการสะสมของความเค้น และการเปลี่ยนแปลงสภาพ ณ จุดสัมผัสระหว่างแขนของเครื่องมือตรวจวัดกับชิ้นงาน ความสามารถของระบบตรวจวัดภาพแบบดิจิตอลเมื่อปรับใช้กับการทดสอบความล้าได้รับการศึกษาโดยการทดสอบความล้าในช่วงความเครียดต่างๆ ของโลหะเชื่อม 3 ชนิดที่อุณหภูมิ 20 °C ผลกระทบและความน่าเชื่อถือของระบบได้รับการตรวจสอบ ผลที่ได้แสดงให้เห็นว่าระบบตรวจวัดภาพแบบดิจิตอลสามารถที่จะนำมาใช้ควบคุมการเปลี่ยนแปลงระยะของชิ้นทดลองในการทดสอบความล้าได้

Abstract

In order to avoid local deformation and stress concentration at contact points between the extensometer and the specimen surface in a strain controlled fatigue test, the digital image measurement system was adapted to measure the displacement of the specimen gage during a fatigue test. Capability of the digital image system for the strain-controlled fatigue testing was studied by preliminary experiments. Low-cycle fatigue tests with various ranges of strain were conducted on solder materials at a constant temperature of 20 °C. The effect of variables in the digital image measurement system on the accuracy and the reliability were discussed. The results confirmed that this system was capable to measure the displacement for strain-controlled fatigue testing.

1. Introduction

In the low cycle fatigue regime, strain-controlled fatigue tests are conducted to obtain basic fatigue characteristics, such as the relationship between strain range and number of cycles to failure (S-N curve). The strain in this regime includes both elastic strain and plastic strain. The information of this testing is essential to mechanical design, material research and development, products performance or failure analysis.

Normally, an extensometer is used for measuring the displacement of the specimen gage in low cycle fatigue tests. The resultant displacement signal is used as feed-back control signal for the fatigue machine. For soft materials such as polymer, tin, silver etc., the local deformation and stress concentration can be induced around the contact point between the extensometer probe and the specimen surface. The cracks have a tendency to initiate earlier in this area, which must influence the specimen life. To avoid this effect, the non-contact strain measuring system should be introduced in a strain-controlled fatigue test of soft materials. The high accuracy digital-image-measurement system in one of the most candidates for the present purpose. Lyons et al.[1] used a digital-image correlation to measure the deformation of flatted surface specimens in tensile tests at high temperatures up to 650 °C. their typical error for strain was 0.0002. Lu et al.[2] used a similar system for thin-walled cylindrical specimens subjected to combined axial and torsional deformations at high temperature. Their technique had accuracy of 3.5 μm for the axial displacement, 0.05 percent in the axial and shear strains and 0.08 percent in the 5 mm x 5 mm computation field for 22.23 mm diameter specimens. McNeill et al.[3] also applied a digital image correlation to measure surface profile. Their results indicated a maximum error of 0.05 mm with camera-to-object distance of 1000 mm.

A non-contact and high accuracy strain-controlled fatigue test system is essential to realize low cycle fatigue tests of soft materials. In this study, the strain controlled fatigue test system with the digital image measurement system was developed. Strain controlled fatigue tests of soft material were also performed at a constant temperature of 20 °C to confirm the accuracy and the reliability of the developed test system.

2. Strain-controlled fatigue test

2.1 System

The CCD camera (charge coupled device camera: Keyence CV-L50) with 50-mm focal length was used in this study. It detects the specimen images and sends these images to the image controller (Keyence CV-550). All of the images are processed in pixel system, a basic unit in image processing. The image controller can process the images, which is composed of approximately 240,000 pixels (512 pixels in the x-direction and 480 pixels in the y-direction). The image are represented in brightness, where 256-levels of brightness are assigned to each pixel. Since this digital image controller can divide one pixel into ten sub-pixels, the detecting ability can be further improved. In order to measure the distance, the image brightness is converted into two digital signals (black and white) by specifying a threshold value. At this stage, all of the pixels are divided into dark and bright groups. The number of pixels in the selected group (black and white) is counted in the image controller. This number of pixels is used for determining the distance. In one second, thirty different images can be processed by the digital image controller. In the present study, two black paper tapes with 0.15 mm thickness are set on the specimen surface to give a gage length. The digital image controller converts the image of black paper tape and gray specimen surface into dark and bright groups. The number of pixels of bright group, which gives the distance of gage length, is counted and used as an

output signal. The working distance between the specimen and the lens of 200 mm was selected to obtain the field of detection of 10 mm or approximately 5,000 sub-pixels in longitudinal direction of the specimen, which covers the gage length. Since the one sub-pixel is the smallest displacement that the digital image controller can detect. Therefore, the accuracy of this system is presumably 2 μm. However, when using this system in real strain controlled fatigue tests, the contrast at the interface between specimen surface and black paper tape is not ideally sharp due to the shadow from the black paper tape edges. Therefore, a circular-shape lamp was set around the lens for evenly illuminating the target to reduce the shadow. However, some errors can not be avoided when running the test in small displacement below 8 μm. Therefore, in the present system, the smallest displacement to control is about 8 μm. The following modification of the system may be recommended: the accuracy of the test can be improved by using bigger lens of CCD camera or reducing the working distance. Also, if two lens are used to detect the upper and lower marks separately, the accuracy and the field of detection will be improved as well.

The output signal from the image controller is in the digital form. Therefore, the D/A converter is used to convert this signal into the appropriate analog signal for the fatigue machine controller. The block diagram of the strain-controlled fatigue test system with digital image measurement system is shown in Fig. 1.

2.2 Discussion on Delay Time

Before using the digital image measurement system in real strain-controlled fatigue tests, the displacement detecting performance was compared with that of extensometer (Shimadzu model: Dynastrain T-508904) on 10 mm gage length specimen under monotonic loading (both tension and compression). The result is shown in Fig. 2. The displacements measured by using both the extensometer and the digital image measurement system are basically similar. The difference are within the ±2 μm range.

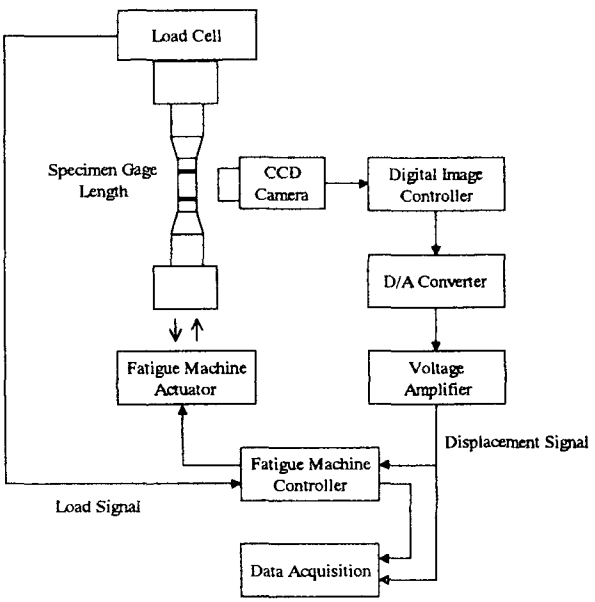

Figure 1. Block diagram of strain-controlled fatigue testing with digital image measurement system

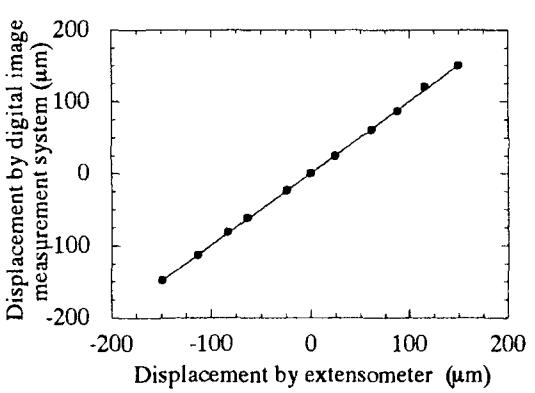

Figure 2. Comparison between displacements measured by using the extensometer and the digital image measurement system

The movements of fatigue machine actuator in triangular and sinusoidal waveforms with different

frequencies were compared with the displacements detected by using the digital image system. The results are shown in Fig. 3. It was found that waveforms and frequencies detected by using the digital image measurement system were in a good agreement with the real movement of the fatigue machine actuator at frequencies lower than 0.1 Hz. However, some delay time of the digital image system was detected at a higher frequency of 0.2 Hz. The time which is required in digital processing is the cause of this delay. Therefore, it does not depend on the frequency or waveform. With the present digital image controller, the magnitude of delay time is approximately 0.7 seconds. Since the fatigue machine controller uses only maximum and minimum value of the feed-back signal to control the movement of actuator. Therefore, this delay time does not affect the actuator oscillation of the fatigue machine. The actuator of the machine still moves with the same frequency and waveform as those of the function generator. However, the delay time has some effects on the data analysis, especially stress-strain loop (hysteresis loop). In a hysteresis loop, stress is calculated from the load signal detected by a load cell, while strain is calculated from the delayed displacement signal detected by the digital image measurement system. This hysteresis loop with delay time does not reproduce the real response of the specimen. Moreover, the incorrect information, such as strain energy , cyclic stiffness, is obtained from the loop. In order to avoid this effect, the compensation of delay time can be made in a personal computer, where the displacement signal is shifted forward by the same amount of delay time. The hysteresis loops with delay time and after compensation of delay time are shown in Fig. 4. The shape of hysteresis loop in both cases are different. It is found that the higher the frequency, the higher the error. Since the delay time does not depend on the test frequency, the delay time effect is significant in the tests at higher frequencies. The percentages of delay time in one cycle for different frequencies are shown in Fig. 5. At 0.1 Hz, the percentages of delay time in one cycle is 7 %, while it is 0.7 % at 0.01 Hz. Therefore, the degree of mismatch between stress and strain is less significant in lower frequency fatigue tests.

From present preliminary examinations, it is found that the developed strain controlled fatigue test system has following advantages: first it does not induce the local deformation and stress concentration due to no contact point for measuring displacement. Therefore, no extra damage occurs other than fatigue damage during fatigue cycles. Secondly, this system has a good accuracy of displacement detection (approximately 8 μm) and 10 mm field of detection which can cover the gage length of the specimen. Third, this system does not require complicated setting and specimen preparation.

3. Low cycle fatigue test

3.1. Experimental Procedures

Three types of solder materials, Ag-Sn eutectic alloy (3.5Ag/96.5Sn), Sn-Pb eutectic alloy (63Sn/37Pb), and Sn-Pb solid solution alloy (5Sn/95Pb) were selected in this strain controlled fatigue tests. All of the materials were supplied in as-cast form. In order to avoid the aging effect, the materials were left to fully aged at room temperature for more than 60 days. The results of Cutongco et al.[4] indicated that the fatigue life increased after a day or two of aging and level off after a week. From bulk solder bars, the fatigue specimens were machined on an NC lathe machine as shown in Fig. 6. The total strain controlled fatigue tests were performed by using a servo-hydraulic fatigue machine (Shimadzu model: EHF-F1) with 2 kN load cell at 55% relative humidity and a constant temperature of 20 ^{o}C. A sinusoidal waveform with 0.1 Hz frequency and R = -1 strain ratio was used for the fatigue tests. The cyclic loading was started from tensile side. The fatigue failure was defined as 25% reduction of the maximum tensile

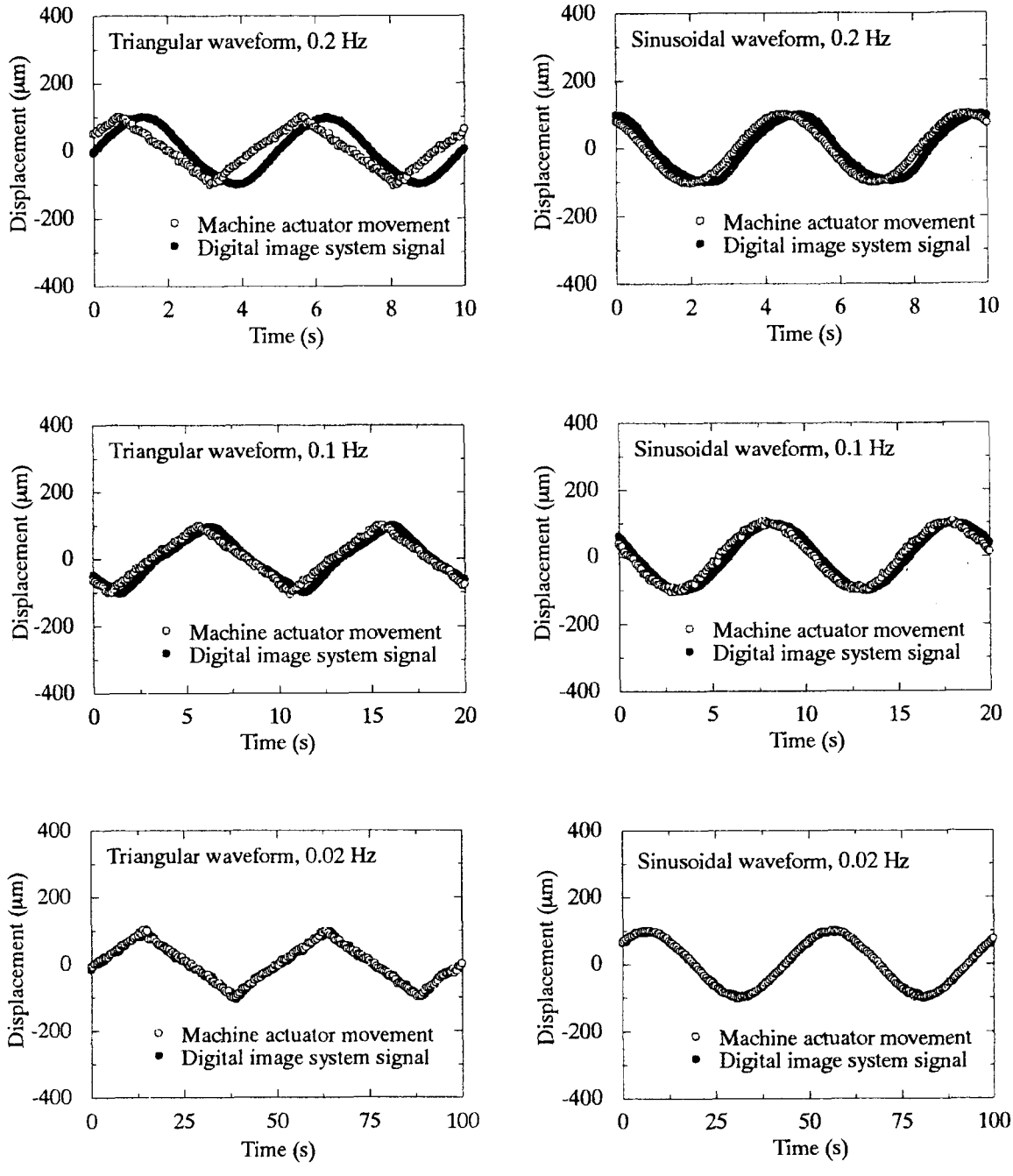

Figure 3. The comparison between the movement of fatigue machine actuator and the digital image measurement system displacement signal at 2.5 % total strain range;

(a) triangular waveform with 0.2, 0.1, 0.02 Hz (b) sinusoidal waveform with 0.2, 0.1, 0.02 Hz

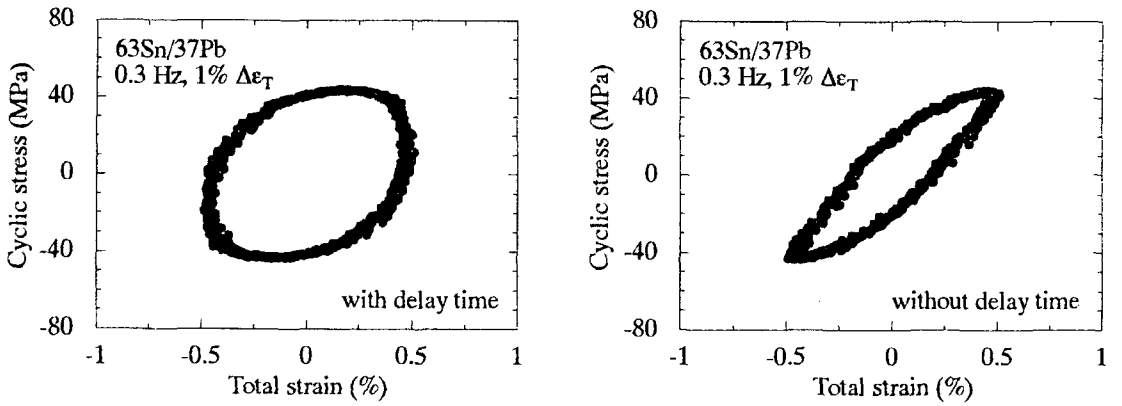

(a)

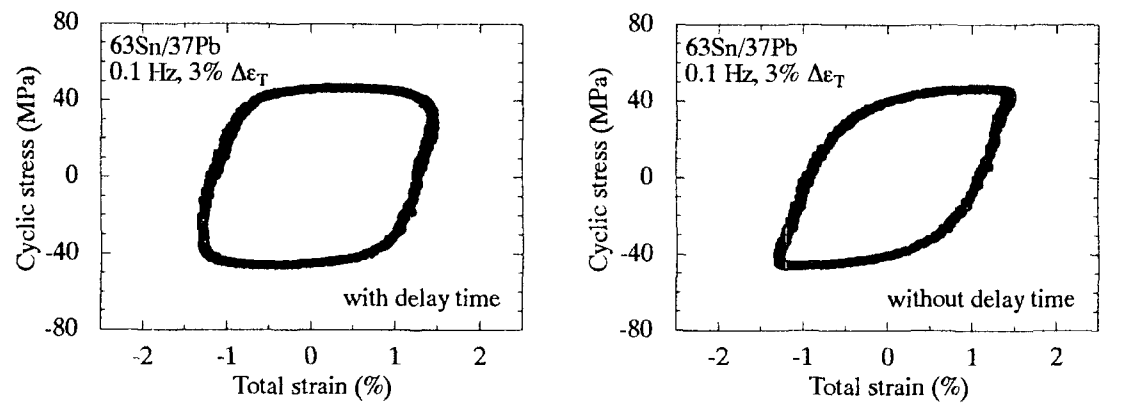

(b)

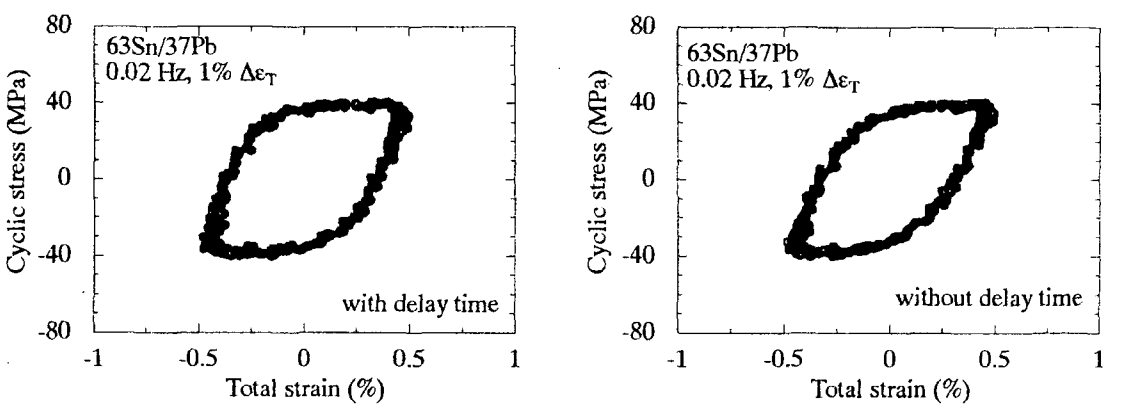

(c)

Figure 4. The comparison between the stress-strain hysteresis loop before and after delay time compensation (a) 1% total strain range with 0.3 Hz, (b) 3% total strain range with 0.1 Hz and (c) 1% total strain range with 0.02 Hz

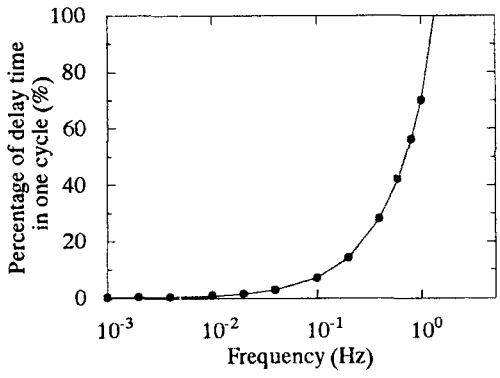

Figure 5. The percentages of delay time in one cycle of different frequencies

load. While running the test, the load, displacement and time were recorded 100 times in each cycle with personal computer-controlled data acquisition. Then, the hysteresis loops were plotted and used for determining plastic strain by subtracting elastic strain from total strain.

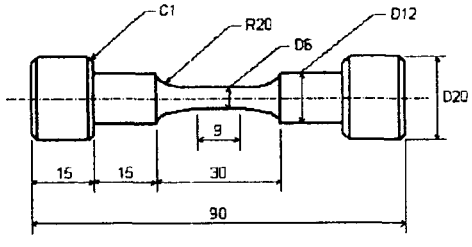

Figure 6. Specimen geometry

3.2. Results

3.2.1. Hysteresis loop

Both the load signal from load cell and the displacement signal from the digital image system were recorded into a personal computer and then were used in calculating cyclic stress and strain in each cycle. Stress-strain hysteresis loops at the first cycle of three types of the materials with different total strain ranges are shown in Fig. 7. The maximum stress in solid solution alloy (5Sn/95Pb) was lower than other two alloys, while the eutectic Sn-Pb alloy (63Sn/37Pb) had the highest maximum stress. In all of three types of solder materials, it was observed that the plastic strain range was almost constant during the test up to failure. The similar behavior was mentioned by Guo et al.[5] The plastic strain range increased with increasing the total strain range. In the same total strain range, the eutectic Sn-Ag alloy (3.5Ag/96.5Sn) had the highest plastic strain range while the eutectic Sn-Pb (63Sn/37Pb) had the lowest one.

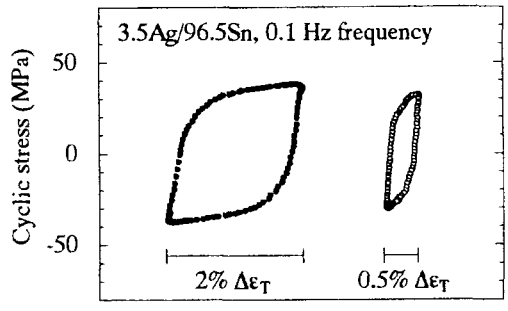

(a)

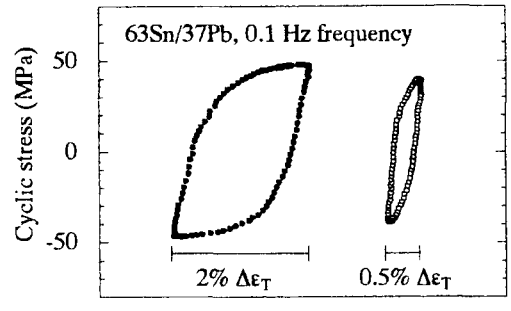

(b)

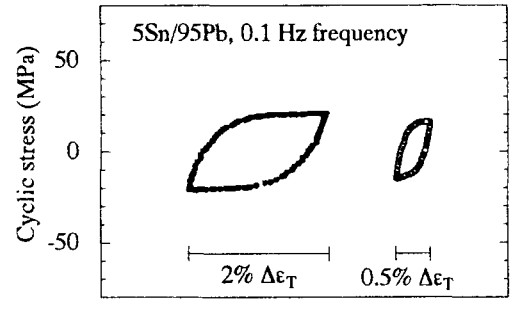

(c)

Figure 7. Cyclic stress-strain hysteresis loops at the beginning of the strain controlled fatigue tests

(a) 3.5Ag/96.5Sn (b) 63Sn/37Pb and (c) 5Sn/95Pb

3.2.2 Cyclic stress-strain relationships

In order to avoid the initial unstable softening behavior, the stress and plastic strain ranges at the half of fatigue life are plotted on log-log scale for three solder materials (3.5Ag/96.5Sn, 63Sn/37Pb and 5Sn/95Pb) in Fig. 8. The data could be fitted by three different lines, which are represented in the following form of equation.

$$\Delta\sigma = A\Delta\varepsilon_p^{\beta} \quad , \qquad (1)$$

where $\Delta\sigma$ is the stress range at the half of fatigue life, $\Delta\varepsilon_p$ is the plastic strain range, A is the cyclic strength coefficient and β is the cyclic strain-hardening exponent. The eutectic Sn-Ag alloy (3.5Ag/96.5Sn) had the highest cyclic strain-hardening exponent (β), while the eutectic Sn-Pb alloy (63Sn/37Pb) had the lowest. Jiang et al.[6] performed the similar study but only for 63Sn/37Pb with strain-gauge extensometer at a constant strain rate of 3.33 x 10^{-3} s^{-1}. They showed that the cyclic strain-hardening exponent (β) of 63Sn/37Pb was 0.09, while in the present study it was 0.18.

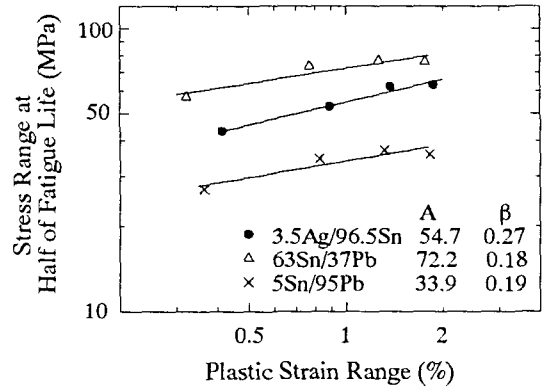

Figure 8. Cyclic stress-strain behavior for 3.5Ag/96.5Sn, 63Sn/37Pb and 5Sn/95Pb

3.2.3 S-N curves

Relationships between total strain range, elastic strain range and plastic strain range and number of cycles to failure for 63Sn/37Pb are shown in Fig. 9. The relationships follow the Coffin-Manson equation:

$$\Delta\varepsilon_p N_f^{\alpha} = \theta \quad , \qquad (2)$$

where $\Delta\varepsilon_p$ is the plastic strain range, N_f is the fatigue life, α is the fatigue ductility exponent and θ is the fatigue ductility coefficient. The slope of the total strain range versus fatigue life curve was smaller than that of the plastic strain range versus fatigue life curve. It was found that the slope of plastic strain range versus fatigue life curve (~ 0.5) was in good agreement with the results obtained by Jiang et al.[6] They conducted the tests with a constant strain rate (3.33 x 10^{-3} s^{-1}), while constant frequency tests (0.1 Hz) were done in the present study. In the present frequency tests, the strain rate varied from test to test (10^{-3} to 4 x 10^{-3} s^{-1}) depending on the total strain range. However, the variation of strain rate in the present experiments was small enough and consequently the fatigue behaviors for both the studied would coincide.

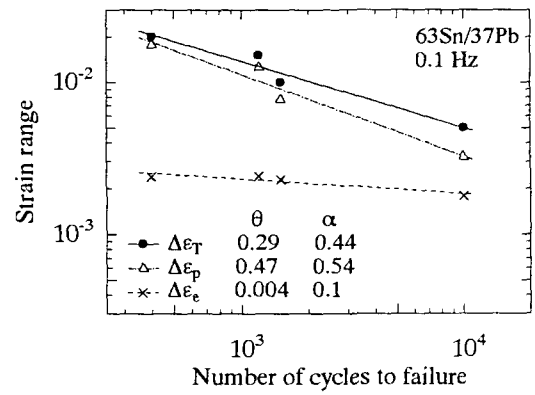

Figure 9. Relationships between total strain range, elastic strain range and plastic strain range versus number of cycles to failure for 63Sn/37Pb at 20 °C and a frequency of 0.1 Hz

Relationship between plastic strain range and fatigue life at a frequency of 0.1 Hz and 20 °C for 3.5Ag/96.5Sn, 63Sn/37Pb and 5Sn/95Pb are shown in Fig. 10. It can be seen from the figure that 63Sn/37Pb

has the shortest fatigue life. The lead free eutectic alloy (3.5Ag/96.5Sn) has the highest low cycle fatigue resistance in the range of the present study.

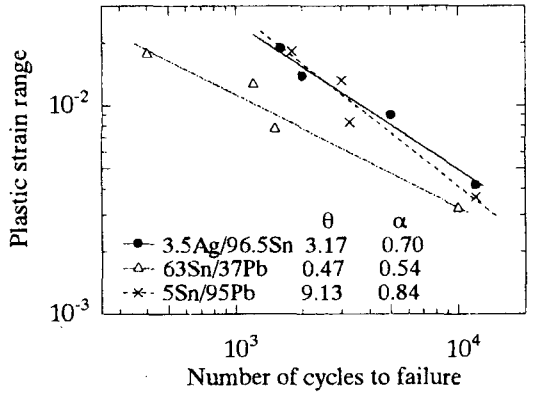

Figure 10. Relationships between plastic strain range and number of cycles to failure for 3.5Ag/96.5Sn, 63Sn/37Pb and 5Sn/95Pb at 20 °C and a frequency of 0.1 Hz

3.3 Discussion

Three kinds of solders showed cyclic softening behavior in all strain range studied here. The load which was required for maintaining a constant total strain range decreased with increasing number of cycles. The reduction started in the first few cycles of the test. The small cracks, which were observed at the beginning of the test, reduce the load bearing area. Therefore, the decrease in load may result from the initiation of small cracks. Based on ultrasonic microscopy evidence, Solomon[7] also proposed that the load reduction is due to fatigue crack nucleation and growth. The pattern of load reduction can be exhibited by a load drop parameter. This parameter is represented in the following form of equation.

$$\phi = 1 - (\Delta P / \Delta P_m) \quad , \qquad (3)$$

where ϕ is the load drop parameter, ΔP is the load range, and ΔP_m is the maximum load range. The relationship between load drop parameter and number

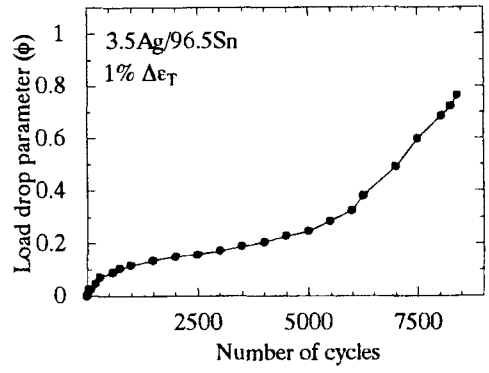

Figure 11. Relationships between load drop parameters and number of cycles at 1% $\Delta\varepsilon_T$ of lead free eutectic alloy (3.5Ag/96.5Sn)

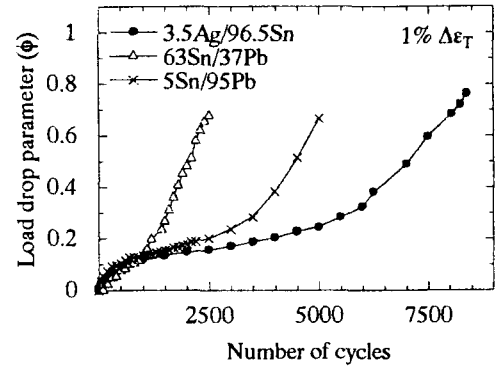

(a)

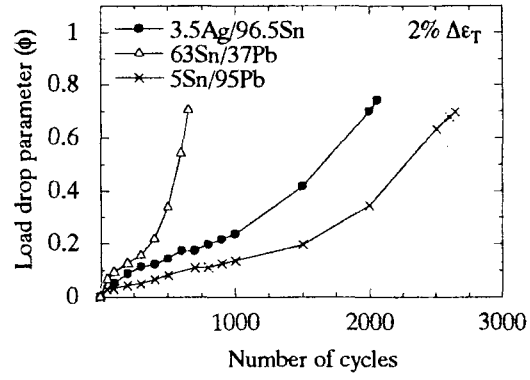

(b)

Figure 12. The load drop parameter curves at (a) 1%, and (b) 2% total strain ranges for three solders

of cycles at 1% $\Delta\varepsilon_T$ for lead free eutectic alloy (3.5Ag/96.5Sn) is shown in Fig. 11. The similar pattern was also observed in other two solder alloys. All load drop parameter curves of the alloys studied here can be divided into three stages; rapid increase stage, steady stage and acceleration stage. Most of the fatigue life is spent in the steady state stage. Therefore, the slope of the load drop parameter curve in the steady state stage reflects the low cycle fatigue life: the fatigue life is longer in case of flatter slope of the steady state stage.

The load drop parameter curves of three solders at 1% and 2% total strain ranges are shown in Fig. 13. In all total strain ranges of the present study, the eutectic Sn-Pb solder (63Sn/37Pb) has the steepest slope of the steady state stage, which corresponds to the lowest low cycle fatigue resistance. The lead free eutectic solder (3.5Ag/96.5Sn) has the most flat slope of the steady state stage at the total strain range below 1.5%, which corresponds to the highest low cycle fatigue resistance.

4. Conclusion

1. A strain controlled fatigue test method without contacts by an extensometer has been developed by using the digital image system. Accuracy of this system is approximately 8 μm in displacement under using 50 mm focal length CCD camera and 200 mm working distance, which is comparable to that for the conventional extensometer. The system has a delay time (0.7 s) due to image processing. However, the effect of delay time is negligible when the frequency is lower than 0.1 Hz.

2. Preliminary low cycle fatigue tests of soft solder materials has been successfully carried out using the developed non-contact strain controlled fatigue test system at a constant temperature of 20 °C.

3. From the test results, the eutectic Sn-Pb solder (63Sn/37Pb) has the lowest low cycle fatigue resistance, while the lead free eutectic solder (3.5Ag/96.5Sn) has the highest one.

4. The slope of the load drop parameter curve in the steady state may correspond to low cycle fatigue life: the fatigue life becomes longer as the slope become flatter.

Reference

[1] J. S. Lyons, J. Liu and M. A. Sutton, "High-temperature Deformation Measurements Using Digital-image Correlation", *Experimental Mechanics*, pp. 64-70, March 1996.

[2] H. Lu, G. Vendroux, and W. G. Knauss, "Surface Deformation Measurements of a Cylindrical Specimen by Digital Image Correlation", *Experimental Mechanics*, vol. 37, no. 4, pp. 433-439, December 1997.

[3] S. R. Mcneill, M. A. Sutton, Z. Miao, and J. Ma, "Measurement of Surface Profile Using Digital Image Correlation", *Experimental Mechanics*, vol. 37, no. 1, pp. 13-20, March 1997

[4] E. C. Cutiongco, S. Vaynman, M. E. Fine, and D. A. Jeannotte, "Isothermal Fatigue of 63Sn-37Pb Solder", *Journal of Electronic Packaging*, Transactions of the ASME, vol. 112, June 1990.

[5] Q. Guo, E. C. Cutiongco, L. M. Keer, and M. E. Fine, "Thermomechanical Fatigue Life Prediction of 63Sn/37Pb Solder", *Journal of Electronic Packaging*, Transactions of the ASME, vol. 114, June 1992.

[6] H. Jiang, R. Hermann, and W. J. Plumbridge, "High-strain fatigue of Pb-Sn eutectic solder alloy", *Journal of Materials Science*, vol. 31, pp. 6455-6461, 1996.

[7] H. D. Solomon, "High and Low Temperature Strain-Life Behavior of a Pb Rich Solder", *Journal of Electronic Packaging*, Transactions of the ASME, vol. 112, June 1990.